Green's function method with energy-independent vertex functions

S. Y. Tsay Tzeng,[1] T. T. S. Kuo,[2,3] Yiharn Tzeng,[2] H. B. Geyer,[4] and P. Navratil[4,5]

[1]*National Taipei Institute of Technology, Taipei, Taiwan 10643, Republic of China*
[2]*Institute of Physics, Academia Sinica, Nankang, Taipei, Taiwan 11529, Republic of China*
[3]*Physics Department, State University of New York at Stony Brook, Stony Brook, New York 11794*
[4]*Institute of Theoretical Physics, University of Stellenbosch, Stellenbosch 7600, South Africa*
[5]*Institute of Nuclear Physics, Czech Academy of Sciences, Řež near Prague, Czech Republic**

In conventional Green's function methods the vertex function Γ is generally energy dependent. However, a model-space Green's function method where the vertex function is manifestly energy independent can be formulated using energy-independent effective interaction theories based on folded diagrams and/or similarity transformations. This is discussed in general and then illustrated for a $1p1h$ model-space Green's function applied to a solvable Lipkin many-fermion model. The poles of the conventional Green's function are obtained by solving a self-consistent Dyson equation and model space calculations may lead to unphysical poles. For the energy-independent model-space Green's function only the physical poles of the model problem are reproduced and are in satisfactory agreement with the exact excitation energies.

In nuclear, atomic, and other many-body calculations, one usually has to resort to some approximation methods, and the Green's function formalism allows some of the most powerful of these methods to be implemented. The particle-hole (ph) Green's function, for example, gives one immediate access to important physical quantities such as excitation energies $\Delta_n = E_n(A) - E_0(A)$ and transition matrix elements $\langle n|X|0\rangle = \langle \Psi_n(A)|X|\Psi_0(A)\rangle$, with the E's and Ψ's denoting, respectively, the energies and wave functions of the many-body system, while X represents any physical transition operator.

A related quantity of central importance in this context is the response function R_X associated with the operator X and defined by

$$R_X(\omega) = \sum_n \frac{\langle \Psi_0|X|\Psi_n\rangle\langle \Psi_n|X^+|\Psi_0\rangle}{\omega - (E_n - E_0) + i0^+}$$
$$- \sum_n \frac{\langle \Psi_0|X|\Psi_n\rangle\langle \Psi_n|X^+|\Psi_0\rangle}{\omega + (E_n - E_0) + i0^+}. \quad (1)$$

It plays an important role in, e.g., nuclear structure theory [1–4] and its construction is intimately linked to Green's function methods.

We now turn to the question of how one actually performs Green's function calculations in order to obtain, for example, excitation energies and transition amplitudes. Denoting the Green's function under consideration by G and the corresponding unperturbed Green's function by F, it is well known [5,6] that G obeys an integral equation, the Dyson equation

$$G(\omega) = F(\omega) + F(\omega)\Gamma(\omega)G(\omega). \quad (2)$$

Here ω is the energy variable, and Γ is the irreducible vertex function, generally dependent on the energy variable ω.

In this work we consider the construction of the Green's function from an effective vertex function Γ_{eff} which is manifestly *energy independent*, that is, the above Dyson equation is reduced to an equation of the form

$$\tilde{G}(\omega) = F(\omega) + F(\omega)\Gamma_{\text{eff}}\tilde{G}(\omega). \quad (3)$$

This form is pursued in the spirit of effective interaction theories [7–9] from which it is well known that there are basically two types of effective interactions—one energy dependent and the other energy independent. In analogy, one would then expect that Green's function methods may be similarly formulated in two ways, with the vertex function being either energy dependent or energy independent. The analogy is even more pronounced when the vertex function $\Gamma(\omega)$ is viewed as a generalized energy-dependent effective interaction [5]. We note that the Green's function $\tilde{G}(\omega)$ of Eq. (3) is not entirely equivalent to G of Eq. (2). The poles of $\tilde{G}$ are also poles of G, but the former are just a subset of the latter. Which poles of G will be reproduced by $\tilde{G}$ depends on the model space choice and also on the particular construction of the effective vertex function Γ_{eff} as discussed in detail below.

A few preliminary remarks are in order here. In practice, Green's function calculations are almost always performed in a restricted model space P, consisting of several single-particle (sp) orbits near the Fermi surface. In fact, the integral equations given above are all viewed as such model space equations here. We first consider the conventional energy-dependent vertex function $\Gamma(\omega)$. Starting from this vertex function, we then discuss how to obtain an energy-independent P-space vertex function Γ_{eff} using the similarity transformation methods of Suzuki and Lee [10,11] and of Navratil *et al.* [12], and also using the folded-diagram method of Krenciglowa and Kuo [13]. An important difference between $\Gamma(\omega)$ and Γ_{eff} is that the former would have poles which, in the case of approximations, will depend on the particular construction, while the latter is independent of ω and obviously does not contain any poles. To investigate

these and other aspects of the present Green's function method, we have analyzed a solvable Lipkin many-fermion model problem [14], using a particle-hole (ph) Green's function analysis.

We first illustrate the derivation of an energy-independent vertex function for the model-space Green's function. As is well known [5], one defines the two-time ph Green's function as

$$G_{php'h'}(t_a - t_b) = \langle \Psi_0 | T\{A_{ph}(t_a) A^+_{p'h'}(t_b)\} | \Psi_0 \rangle$$
$$- \langle \Psi_0 | A_{ph} | \Psi_0 \rangle \langle \Psi_0 | A^+_{p'h'} | \Psi_0 \rangle. \quad (4)$$

Ψ_0 denotes the ground state of the system and the A's are the particle-hole operators

$$A^+_{p'h'}(t_b) = e^{iHt_b} A^+_{p'h'} e^{-iHt_b},$$

$$A^+_{p'h'} = a^+_{p'} a_{h'},$$

$$A_{ph}(t_a) = [A^+_{ph}(t_a)]^+. \quad (5)$$

Here H is the full Hamiltonian. The Green's function (4) has the Lehmann representation

$$G_{php'h'}(\omega) = \sum_{n \neq 0} \frac{X_n(ph) X^*_n(p'h')}{\omega - \Delta_n + i0^+}$$
$$- \sum_{n \neq 0} \frac{Y^*_n(ph) Y_n(p'h')}{\omega + \Delta_n - i0^+},$$

$$X_n(ph) = \langle \Psi_0 | A_{ph} | \Psi_n \rangle,$$

$$Y_n(ph) = \langle \Psi_0 | A^+_{ph} | \Psi_n \rangle. \quad (6)$$

To calculate Δ_n, X_n, and Y_n, one solves the model-space secular equation [5,6]

$$\sum_{p''h''} \{(\epsilon_p - \epsilon_h) \delta_{ph,p''h''} + (n_p - n_h) \Gamma_{php''h''}(\omega)\} X_n(p''h'')$$
$$= \Delta_n(\omega) X_n(ph), \quad (7)$$

with the self-consistent condition $\omega = \Delta_n$. The solutions of the above equation are paired, with both Δ_n and $-\Delta_n$ solutions; wave functions X_n correspond to positive Δ_n and Y_n to negative Δ_n.

When the above equations are solved within a chosen model space P, intermediate states of the vertex function must be orthogonal to P, in other words, belong to the complement space Q with $P + Q = 1$. To illustrate this, we use a restricted $1p1h$ model space, and show some low-order diagrammatic contributions to Γ in Fig. 1. Diagrams $A1$ and $B1$ are first order in V, the interaction part of the Hamiltonian, and these two diagrams are ω independent. Diagrams $A2 - A6$ are ω dependent, and are of the general form $PVQ[1/(\omega - H_0)]QVP$ where H_0 represents the noninteracting part of the Hamiltonian. Here Q denotes the space spanned by the $2p2h$ states.

Suppose now we use an effective interaction V_{eff}, constructed from a $1p1h$ model space. Then the above diagrams, $A2 - A6$, are of the form $PV_{\text{eff}}Q[1/(\omega - H_0)]/QV_{\text{eff}}P$. In ef-
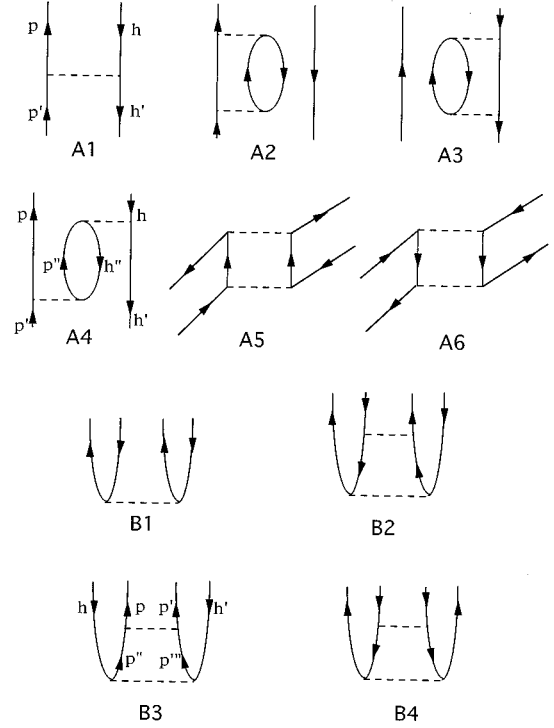

FIG. 1. Diagrams of the particle-hole vertex functions.

fective interaction theories, it is well known that V_{eff} can be derived using a similarity-transformation approach (see [11] and references quoted therein). The resulting V_{eff} can be constructed to be energy independent and satisfies the decoupling condition $QV_{\text{eff}}P = 0$. (This follows from the requirement $QH_{\text{eff}}P = 0$, where H_{eff} is the transformed Hamiltonian and the effective interaction V_{eff} is defined as $V_{\text{eff}} = H_{\text{eff}} - H_0$.) In an analogous way, one can also obtain an energy-independent general effective operator by way of similarity transformations [12], in which case one has the dual decoupling conditions of $QV_{\text{eff}}P = PV_{\text{eff}}Q = 0$. These considerations may now be applied to the above vertex-function diagrams, whence diagrams $A2 - A6$ vanish because of the decoupling condition, while diagram $A1$ becomes $\langle ph^{-1} | V_{\text{eff}} | p'h'^{-1} \rangle$. (Note that in the present case we take P as composed of $1p1h$ basis states, with Q restricted to $2p2h$ states.) The decoupling conditions do not ensure that diagrams $B2 - B4$ vanish, but by employing a "time-blocking" formalism, these diagrams become ω independent [6]. For example, diagram $B3$ is of the form $V_{\text{eff}}(1/e)V_{\text{eff}}$ where $e = \epsilon(h) + \epsilon(h') - \epsilon(p'') - \epsilon(p''')$, where the ϵ's are single-particle energies defined by H_0.

Thus, by applying the above effective interaction and effective operator approaches, one obtains a Green's function whose vertex function Γ_{eff} is explicitly energy independent. Namely, we have a Green's function secular equation of the form

$$\sum_{p''h''} \{(\epsilon_p - \epsilon_h) \delta_{ph,p''h''} + (n_p - n_h) \langle ph | \Gamma_{\text{eff}} | p''h'' \rangle\} \bar{X}_n(p''h'')$$
$$= \bar{\Delta}_n \bar{X}_n(ph). \quad (8)$$

It is worthwhile to note that a similar result holds in the case of the one-body Green's function where the mass op-

erator M replaces the vertex function, e.g., in derivations of the optical-model potential. In most formalisms, M is energy dependent and hence so is the optical-model potential. However, by way of a folded-diagram factorization, Kuo, Lee, and Osterfeld [15] have obtained an energy-independent mass operator for the one-body Green's function, based on which an energy-independent optical-model potential may be constructed. The present work is an extension of their work to the case of two-body Green's functions.

To calculate the energy-independent vertex function, we first derive an energy-independent effective interaction for a $1p1h$ model space, using a folded-diagram method [8]. We use diagrams $A1-A6$ to calculate the $\hat{Q}$ box and the effective interaction is then given by the folded-diagram series $V_{\mathrm{eff}} = \hat{Q} - \hat{Q}\int\hat{Q} + \hat{Q}\int\hat{Q}\int\hat{Q} - \cdots$. In this way the contributions of diagrams $A2-A6$ are excluded from Γ_{eff} as they are already absorbed into diagram $A1$. Only diagrams $A1$ and $B1-B4$ may now contribute to Γ_{eff}. The resulting Γ_{eff} is clearly ω independent. To sum the folded diagrams contained in V_{eff} we have employed two iteration methods, the Lee-Suzuki (LS) [10] method and the Krenciglowa-Kuo (KK) [13] method.

Denoting the dimension of the $1p1h$ space by d, it follows that Eq. (8) can have only d solutions for the excitation energies $\bar{\Delta}_n$. In contrast, in Eq. (7) $\Delta_n(\omega)$ is energy dependent and from the self-consistent condition $\omega = \Delta_n(\omega)$ more than d solutions may result, even though the P space is of the same dimension d. The model-space Green's function defined by Γ_{eff} has only d poles, while the original Green's function may in general have more poles. The transition amplitudes derived from Γ_{eff} are now obtained as the P-space transition amplitudes $\bar{X}_n(ph) = \langle P\Psi_0|A_{ph}|P\Psi_n\rangle$ and $\bar{Y}_n(ph) = \langle P\Psi_0|A_{ph}^+|P\Psi_n\rangle$.

To illustrate and compare the two Green's function methods, one with energy-dependent and the other with energy-independent vertex function, we have carried out some model calculations. The model considered is an extended [16] Lipkin model, with the Hamiltonian

$$H = H_0 + H_{\mathrm{int}},$$

$$H_0 = \frac{\Delta}{2}\sum_{p\sigma}\sigma a_{p\sigma}^+ a_{p\sigma},$$

$$
\begin{aligned}
H_{\mathrm{int}} = &\frac{V}{2}\sum_{pp'\sigma} a_{p\sigma}^+ a_{p'\sigma}^+ a_{p'-\sigma} a_{p-\sigma} \\
&+ \frac{W}{2}\sum_{pp'\sigma} a_{p\sigma}^+ a_{p'-\sigma}^+ a_{p'\sigma} a_{p-\sigma} \\
&+ \frac{U}{2}\sum_{pp'\sigma}(a_{p\sigma}^+ a_{p'\sigma}^+ a_{p'-\sigma} a_{p\sigma} + a_{p\sigma}^+ a_{p'-\sigma}^+ a_{p'\sigma} a_{p\sigma}).
\end{aligned}
$$

(9)

It is a two-level model, with its single-particle levels labeled by $\sigma = +, -$. The degeneracy of each level is p, and the single-particle energies are $\pm(1/2)\Delta$. The interaction part has three terms with strengths V, W, and U, respectively. (The original Lipkin model [14] has the V term only.)
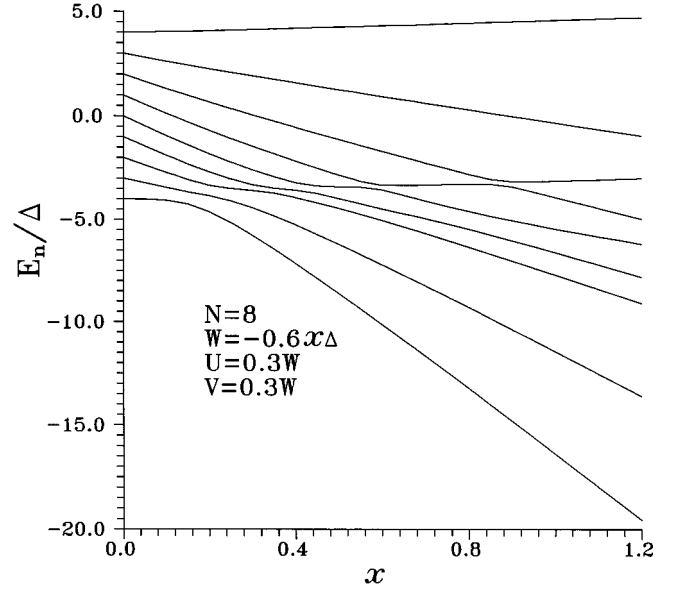

FIG. 2. A typical exact energy spectrum of our model problem.

We consider the "closed-shell" situation with $N = p$, where N denotes the number of particles, and focus on those states with maximum J. Consider for example $N = p = 8$: each particle has spin 1/2, and thus $J_{\max} = 4$. The lowest unperturbed $J = 4$ state is a closed-shell state with all eight particles in the $\sigma = -1$ orbit.

Exact matrix diagonalization for the above model problem can be readily performed. An interaction strength parameter x is introduced, namely the Hamiltonian is written as $H = H_0 + xH_{\mathrm{int}}$ and in Fig. 2 we display an exact energy spectrum for the $J = 4$, $N = p = 8$ states mentioned above.

The lowest level in the figure is the ground state with energy E_0, and the Green's function method is now alternatively used to calculate the excitation energies. First we employ the conventional energy-dependent Green's function method, Eq. (8). For the vertex function, we include all the diagrams listed in Fig. 1. As usual, we first perform a Hartree-Fock (HF) calculation, and the resulting HF basis and single-particle energies are then employed to calculate these diagrams and in setting up Eq. (8). The eigenvalues Δ_n are calculated as a function of ω and are plotted in Fig. 3. The slanted line in the figure is $\omega = \Delta_n$, and the self-consistent solutions of Eq. (8) are given by the intersection points a, b, $c1$, and $c2$. These four points are associated with the excitation energies $E_n - E_0$, $n = 1, \ldots, 4$.

Next we turn to the energy-independent Green's function method of Eq. (9). We first calculate the model-space $(1p1h)$ energy-independent effective interaction using both the Lee-Suzuki (LS) [10] and the Krenciglowa-Kuo (KK) [13] iteration methods. For the Q box, we include diagrams $A1-A6$ of Fig. 1. Again we first carry out a HF calculation and use the HF basis for subsequent calculations. The effective interaction is derived in two steps. First we include all these six diagrams in the Q box and sum the entire Q box folded diagram series, denoting the resulting effective interaction as $U_{\mathrm{eff}}(1+2)$. We then repeat the calculation, including only the one-body diagrams $A1-A3$ in the Q box. The resulting effective interaction is denoted as $U_{\mathrm{eff}}(1)$. The final effective interaction V_{eff}, which is energy independent and two-body
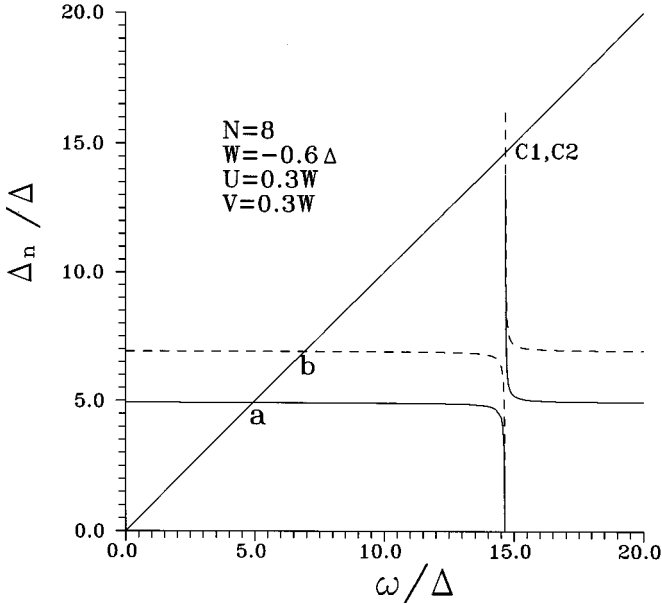
FIG. 3. Graphical solution of Eq. (8). The self-consistent solutions are given by the intersection points a, b, $c1$, and $c2$.

FIG. 4. Solutions of Eq. (9) with the energy-independent vertex function Γ_{eff} given by the LS method (+) and by the KK method ($\bigcirc$). The exact results (solid line) are also shown.

valence linked, is given by the difference $U_{\mathrm{eff}}(1+2) - U_{\mathrm{eff}}(1)$. The energy-independent vertex function Γ_{eff} is determined by diagrams $A1$ and $B1-B4$, where each dashed line represents a V_{eff} vertex.

Our results are shown in Fig. 4, where the excitation energies given by Eq. (9) are compared with the exact results. For a wide range of the interaction strength, the excitation energies given by the KK and LS energy-independent effective interactions are both in very good agreement with the exact values. Our model space is one dimensional, and hence Eq. (9) only gives one excitation energy, identified as the first excitation energy $\Delta_1 = (E_1 - E_0)$.

In contrast, Eq. (8) of the conventional energy-dependent method has four solutions, although the dimension of the $1p1h$ model space is still one. These three solutions are indicated by the intersection points a, b, $c1$, and $c2$ of Fig. 3. Note that points $c1$ and $c2$ practically coincide. The energy given by point a is a physical solution, in very good agreement with the exact excitation energy $(E_1 - E_0)$. The excitation energies given by the other intersection points, however,
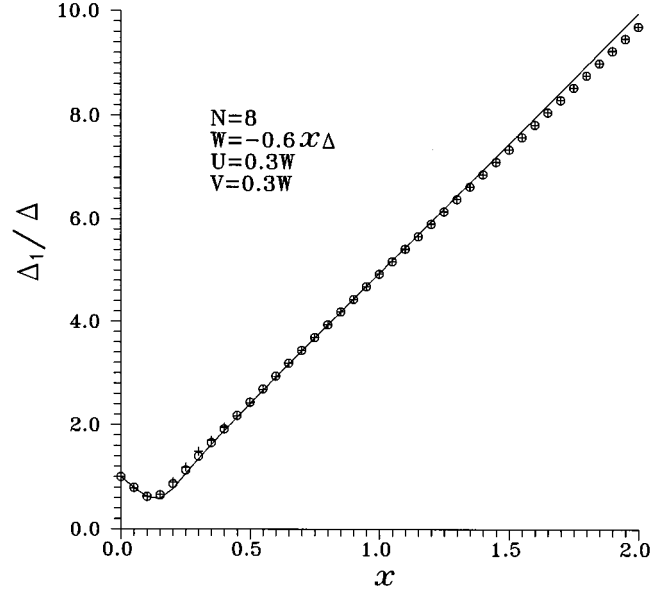
do not seem to correspond to any of the exact excitation energies and are thus considered unphysical, at least within the present context. In Table I we summarize the above results as obtained from Eqs. (8) and (9) in comparison with the exact results.

Particularly the poles given by points $c1$ and $c2$ are worth attention; they are closely related to the poles of the vertex function $\Gamma(\omega)$ as elaborated below. One usually calculates $\Gamma(\omega)$ by a low-order perturbation method, as in the present calculation of $\Gamma(\omega)$ from the diagrams of Fig. 1. Consequently $\Gamma(\omega)$ will have a pole at QH_0Q, namely at the unperturbed energies of the intermediate states appearing in the low-order diagrams included. For example, diagram $A4$ has a pole at its intermediate-state energy $[\epsilon(p) + \epsilon(p') - \epsilon(h) - \epsilon(h')]$.

The position of this pole is dependent on the single-particle spectrum employed, and is also dependent on the range of the intermediate states we choose to include. Because of the sensitive energy dependence of Δ_n near the

TABLE I. Comparisons of $\Delta_n(\omega)$, solutions given by Eq. (8), and Δ_1 (KK), Δ_1 (LS), those given by Eq. (9), with the exact results (Δ_n^{ex}). Listed in the last row are the HF single-particle energy differences. [All entries of energies are in units of Δ of Eq. (9).]

	$N=8$			$N=50$		
NW/Δ	-0.2	-2.0	-4.8	-0.2	-2.0	-6.0
Δ_1^{ex}	0.827	1.971	4.944	0.806	2.281	7.026
Δ_2^{ex}	1.704	3.364	8.674	1.620	4.483	13.832
Δ_3^{ex}	2.632	3.770	9.772	2.443	6.606	20.414
Δ_1 (KK)	0.827	2.005	4.929	0.809	2.248	6.902
Δ_1 (LS)	0.826	2.095	4.931	0.806	2.299	7.013
$\Delta_1(\omega) = \omega$	0.827	2.006	4.929	0.806	2.287	7.037
$\Delta_2(\omega) = \omega$	1.027	2.918	6.916	1.007	3.184	9.460
$\Delta_{3,4}(\omega) = \omega$	2.058	6.191	14.678	2.020	6.496	19.086
$\epsilon_2^{\mathrm{HF}} - \epsilon_1^{\mathrm{HF}}$	1.027	3.086	7.334	1.007	3.208	9.538

poles of $\Gamma(\omega)$, as illustrated by the lines near point $c1$ or $c2$ of Fig. 3, it is quite likely that the Green's function will always have a pole in close vicinity of the pole of the vertex function $\Gamma(\omega)$. These type of poles of G seem to be clearly unphysical, as they are determined predominantly by the approximation method we choose for calculating the vertex function.

From the Dyson equation (2) for the energy-dependent Green's function, it follows that $\Gamma = 1/F - 1/G$. The poles of the vertex function Γ are thus determined by the true Green's function G; in fact they correspond to the zeroes of G. If, as is usually done in practice, the poles of Γ are determined from some perturbation method, Γ, and consequently the Green's function G, will acquire unphysical poles if one uses an energy-dependent Green's function method, as we have illustrated. These type of unphysical poles of G may, however, be avoided if one employs the energy-independent Green's function method discussed in the present work.

[1] B. Froi and C. N. Papanicolas, Annu. Rev. Nucl. Part. Sci. **37**, 133 (1987).

[2] S. Drozdz, S. Nishizaki, J. Speth, and J. Wambach, Phys. Rep. **190**, 1 (1990).

[3] S. Krewald, K. Nakayama, and J. Speth, Phys. Rep. **161**, 104 (1988).

[4] G. F. Bertsch and S. F. Tsai, Phys. Rep. **18**, 125 (1975).

[5] S. S. Wu and T. T. S. Kuo, Nucl. Phys. **A430**, 110 (1984).

[6] T. T. S. Kuo and Yiharn Tzeng, Int. J. Mod. Phys. E **3**, 523 (1994).

[7] P. J. Ellis and E. Osnes, Rev. Mod. Phys. **49**, 777 (1977).

[8] T. T. S. Kuo and E. Osnes, *Folded-Diagram Theory of Effective Interaction in Nuclei, Atoms and Molecules*, Lecture Notes in Physics Vol. 364 (Springer-Verlag, Berlin, 1990).

[9] T. T. S. Kuo, in *Topics in Nuclear Physics*, edited by T. T. S. Kuo and S. M. Wong, Lecture Notes in Physics Vol. 144 (Springer-Verlag, Berlin, 1981), p. 248.

[10] S. Y. Lee and K. Suzuki, Phys. Lett. **91B**, 173 (1980); K. Suzuki and S. Y. Lee, Prog. Theor. Phys. **64**, 2091 (1980).

[11] K. Suzuki, R. Okamoto, P. J. Ellis, and T. T. S. Kuo, Nucl. Phys. **A567**, 576 (1994).

[12] P. Navratil, H. B. Geyer, and T. T. S. Kuo, Phys. Lett. B **315**, 1 (1993).

[13] E. M. Krenciglowa and T. T. S. Kuo, Nucl. Phys. **A235**, 171 (1974).

[14] H. J. Lipkin, N. Meshkov, and A. J. Glick, Nucl. Phys. **62**, 188 (1965).

[15] T. T. S. Kuo, F. Osterfeld, and S. Y. Lee, Phys. Rev. Lett. **45**, 786 (1980).

[16] M. R. Anastasio, T. T. S. Kuo, T. Engeland, and E. Osnes, Nucl. Phys. **A271**, 109 (1976).